An Empirical Demonstration of Unsupervised Machine Learning in Species Delimitation

Shahan Derkarabetian[1,2], Stephanie Castillo[2,3], Peter K. Koo[4], Sergey Ovchinnikov[5], Marshal Hedin[2]

1. Department of Organismic and Evolutionary Biology, Museum of Comparative Zoology, Harvard University, Cambridge, MA 02138

2. Department of Biology, San Diego State University, San Diego, CA 92182

3. Department of Entomology, University of California, Riverside, Riverside, CA 92521

4. Howard Hughes Medical Institute, Department of Molecular and Cellular Biology, Harvard University, Cambridge, MA 02138

5. Center for Systems Biology, Harvard University, Cambridge, MA 02138

Corresponding author: Shahan Derkarabetian

Department of Organismic and Evolutionary Biology

Museum of Comparative Zoology

Harvard University

Cambridge, MA 02138

sderkarabetian@gmail.com

ABSTRACT

One major challenge to delimiting species with genetic data is successfully differentiating species divergences from population structure, with some current methods biased towards overestimating species numbers. Many fields of science are now utilizing machine learning (ML) approaches, and in systematics and evolutionary biology, supervised ML algorithms have recently been incorporated to infer species boundaries. However, these methods require the creation of training data with associated labels. Unsupervised ML, on the other hand, uses the inherent structure in data and hence does not require any user-specified training labels, thus providing a more objective approach to species delimitation. In the context of integrative taxonomy, we demonstrate the utility of three unsupervised ML approaches, specifically random forests, variational autoencoders, and t-distributed stochastic neighbor embedding, for species delimitation utilizing a short-range endemic harvestman taxon (Laniatores, *Metanonychus*). First, we combine mitochondrial data with examination of male genitalic morphology to identify a priori species hypotheses. Then we use single nucleotide polymorphism data derived from sequence capture of ultraconserved elements (UCEs) to test the efficacy of unsupervised ML algorithms in successfully identifying a priori species, comparing results to commonly used genetic approaches. Finally, we use two validation methods to assess a priori species hypotheses using UCE data. We find that unsupervised ML approaches successfully cluster samples according to species level divergences and not to high levels of population structure, while standard model-based validation methods over-split species, in some instances suggesting that all sampled individuals are distinct species. Moreover, unsupervised ML approaches offer the benefits of better data visualization in two-dimensional space and the ability to accommodate various data types. We argue that ML methods may be better suited for species delimitation

45 relative to currently used model-based validation methods, and that species delimitation in a truly
46 integrative framework provides more robust final species hypotheses relative to separating
47 delimitation into distinct "discovery" and "validation" phases. Unsupervised ML is a powerful
48 analytical approach that can be incorporated into many aspects of systematic biology, including
49 species delimitation. Based on results of our empirical dataset, we make several taxonomic
50 changes including description of a new species.
51
52
53 **Key Words:** Random Forest, t-SNE, Variational Autoencoders, ultraconserved elements,
54 integrative taxonomy, Opiliones

Modern species delimitation is becoming increasingly objective relying on, for example, statistical thresholds and/or clustering algorithms to identify species in multivariate morphological space (e.g., Ezard et al. 2010; Seifert et al. 2014), or using the multispecies coalescent to identify the boundary between population and species level divergences using genetic data (e.g., Yang and Rannala 2010). Similarly, species delimitation is becoming increasingly integrative, combining multiple data types in a reciprocally-illuminating framework providing more robust final species hypotheses (Dayrat 2005; Schlick-Steiner et al. 2010). The empirical process of delimiting species has been portrayed by some authors as occurring in two separate phases (Carstens et al. 2013): a discovery phase where a priori hypotheses are formed based on one or more data types, followed by a validation phase where species hypotheses are further tested using an independent dataset, typically nuclear genetic data. Of utmost interest in using genetic data in species delimitation, whether as validation or otherwise, is successfully distinguishing population structure from species level divergences. Recently, Sukumaran and Knowles (2017) demonstrated that the multispecies coalescent model will support population level divergences, an assertation previously demonstrated empirically (e.g., Niemiller et al. 2012; Hedin et al. 2015).

Across many fields of science, a great deal of attention has been given to machine learning (ML) approaches, where an algorithm can be trained to make future decisions without user input. Recently, ML methods like random forest (RF; Breiman 2001) have been incorporated into systematics and evolutionary biology, with applications in barcoding (e.g., Austerlitz et al. 2010), environmental DNA metabarcoding (e.g., Cordier et al. 2018), population genetics (e.g., Schrider and Kern 2016; Schrider and Kern 2018), and predicting cryptic diversity (Espíndola et al. 2016). Most relevant here is the use of RF in phylogeographic model selection

(Pudlo et al. 2016; Smith et al. 2017) and speciation/species delimitation (Pei et al. 2018; Smith and Carstens 2018) where it can be used as a validation tool distinguishing among multiple user-specified models given a priori information about the training data. Similarly, non-RF ML approaches have been used to model biogeographic processes (Sukumaran et al. 2015). In these examples a *supervised* ML approach is used, where simulated datasets based on user-specified priors are used as training data, and a classifier is built to choose among different models or species hypotheses given observed data. For example, the recently developed RF-based species delimitation program CLADES (Pei et al. 2018) approaches species delimitation as a classification issue. Here, a two-species model with varying divergence times and population sizes, with or without migration, is used to simulate the training datasets for classifier construction. Multiple population genetic summary statistics are computed for labeled training data and observed data with species hypotheses defined a priori. These statistics are used as variables to determine support for a priori species distinctiveness in the observed data.

While supervised approaches are indeed powerful, unsupervised ML may also be a useful approach to aid in species delimitation using the inherent structure in the data to cluster samples. Unsupervised ML can be conducted without a priori hypotheses regarding the underlying evolutionary model, population parameters, number of species, species assignment, or levels of parameter divergence needed to classify samples as different species. In unsupervised RF, the training data is a synthetic dataset based on the observed data representing the null hypothesis of no structure, and a classifier is built to distinguish the synthetic and observed datasets, thus uncovering underlying structure (if present) in the observed data. Many unsupervised ML algorithms for high-dimensionality data intrinsically perform reduction to a lower dimensional space, where the underlying data structure can be visualized. For example, Oltaenu et al. (2013)

take an unsupervised ML approach to visualizing and clustering barcode data via nonlinear dimension reduction and projection methods using multidimensional scaling and self-organizing maps. They show that these approaches successfully clustered named and unnamed species and suggested the possibility of undescribed species.

Many ML algorithms can be executed in an unsupervised manner, and while dimensionality reduction methods like principal components analyses and clustering algorithms like k-means are widely considered to be ML, we focus on three unsupervised ML approaches chosen to represent a diversity of ML algorithm types including one that has yet to be used in the field of systematics (Table 1): Random Forests (RF; Breiman 2001), Variational Autoencoders (VAE; Kingma and Welling 2013), and t-Distributed Stochastic Neighbor Embedding (t-SNE; van der Maaten and Hinton 2008). RF is an ensemble learning method that relies on classification trees and tree bagging (Breiman 1996; 2001). In RF most importantly, in a given classification tree if two samples appear at the same terminal node their "proximity score" is increased by one. Proximity scores for all pairs are averaged over bootstrap replicates to produce a final proximity matrix, which can be used in multidimensional scaling (MDS) and clustering. A Variational Autoencoder is a Bayesian approach that learns a distribution of the data using latent variables. It does so in two stages: 1) inference of the posterior distribution of latent variables and 2) generation of data sampled from a given set of latent values. Both stages are approximated by neural networks and optimized simultaneously via unsupervised learning. Widely-used in diverse fields (e.g., Bauer et al. 2015; Yoshida et al. 2016; Mallet et al. 2017), t-SNE is a non-linear dimensionality reduction algorithm that attempts to preserve probability distributions of distances among samples within a cluster but repels samples that are in different clusters in lower-dimensional space.

Table 1. Comparison of unsupervised machine learning methods used in this study.

Method	Purpose	Approach used	General algorithm	Relevant output
Random Forest (RF)	Classification and regression	Supervised Unsupervised	Ensemble method that grows many classification trees based on training data, runs input data down trees, and the classification with the most votes is chosen.	Proximity matrix
Variational Autoencoder (VAE)	Generative model	Unsupervised	Compresses data through multiple encoding layers into latent variables, then un-compresses latent variables through multiple decoder layers into reconstructed data. Learns the marginal likelihood distribution of the data using latent variables.	Latent variables (two-dimensional encoding)
t-Distributed Stochastic Neighbor Embedding (t-SNE)	Data embedding and visualization	Unsupervised	Constructs probability distribution of sample pairs, then minimizes divergence between high dimensional space and low dimension embedding, such that similar pairs are embedded nearby while dissimilar pairs are repelled.	Low dimensional embedding

The purpose of this study was, in the context of integrative taxonomy, to explore and demonstrate the utility of unsupervised ML approaches in aiding species delimitation through successful identification of clusters corresponding to species, as corroborated by other traditional methods. First, in the discovery phase, we combine phylogenetic analysis of mitochondrial cytochrome oxidase subunit I (COI) and examination of morphology to generate a priori species hypotheses. Then, using single nucleotide polymorphisms (SNPs) derived from sequence capture of ultraconserved elements (UCEs) we demonstrate the ability of unsupervised ML approaches to successfully cluster identified a priori species, comparing three unsupervised ML approaches to commonly used methods. Finally, using UCE-derived SNPs and loci we validate species hypotheses using a standard delimitation method and a novel RF-based approach. We also demonstrate the utility of unsupervised ML on two previously published datasets.

MATERIALS AND METHODS

Study System

For this study we utilized a short-range endemic (SRE; Harvey 2002) arachnid taxon in the order Opiliones (commonly called harvestmen). SRE taxa tend to have low dispersal ability and high ecological constraints, which leads to high population genetic structure and allopatric distributions, likely driven by niche conservatism (Wiens and Graham 2005). These biological characteristics make SRE taxa ideal candidates for species delimitation analyses, with high probability for new species discovery. Studies in SRE harvestmen (and SRE taxa in general) tend to show a great deal of underestimated diversity with numerous harvestmen species still being described even from well-studied areas (e.g., Derkarabetian and Hedin 2014; DiDomenico and Hedin 2016; Starrett et al. 2016; Emata & Hedin 2016).

The Pacific Northwest endemic genus *Metanonychus* Briggs, 1971 is a cryophilic harvestman that prefers moist forests, typically found underneath rotting logs/bark and in leaf litter. The genus and all species/subspecies were described by Briggs (1971), and currently includes three species: *M. idahoensis*, *M. setulus* with five subspecies (*setulus*, *mazamus*, *cascadus*, *navarrus*, and *obrieni*), and *M. oregonus* with two subspecies (*oregonus* and *nigricans*) (Fig. 1). *Metanonychus* is an ancient lineage; in a recent phylogenomic analysis of the superfamily Travunioidea (which contains *Metanonychus*), more genetic divergence is seen between the two samples of *Metanonychus* than in divergences between the vast majority of pairs of sister genera across all Travunioidea (Derkarabetian et al. 2018). Despite the ancient origin of this group, relatively few species were described, even though all "subspecies" are easily differentiated based on apparently fixed differences in male genitalic morphology (Briggs 1971). Recent systematic studies on related taxa corroborate the conservative nature of

subspecies in these SRE harvestmen (Derkarabetian and Hedin 2014). As such, and more importantly, we consider *Metanonychus* species limits relatively straightforward where the species are "obvious" making this an excellent system to test ML approaches.

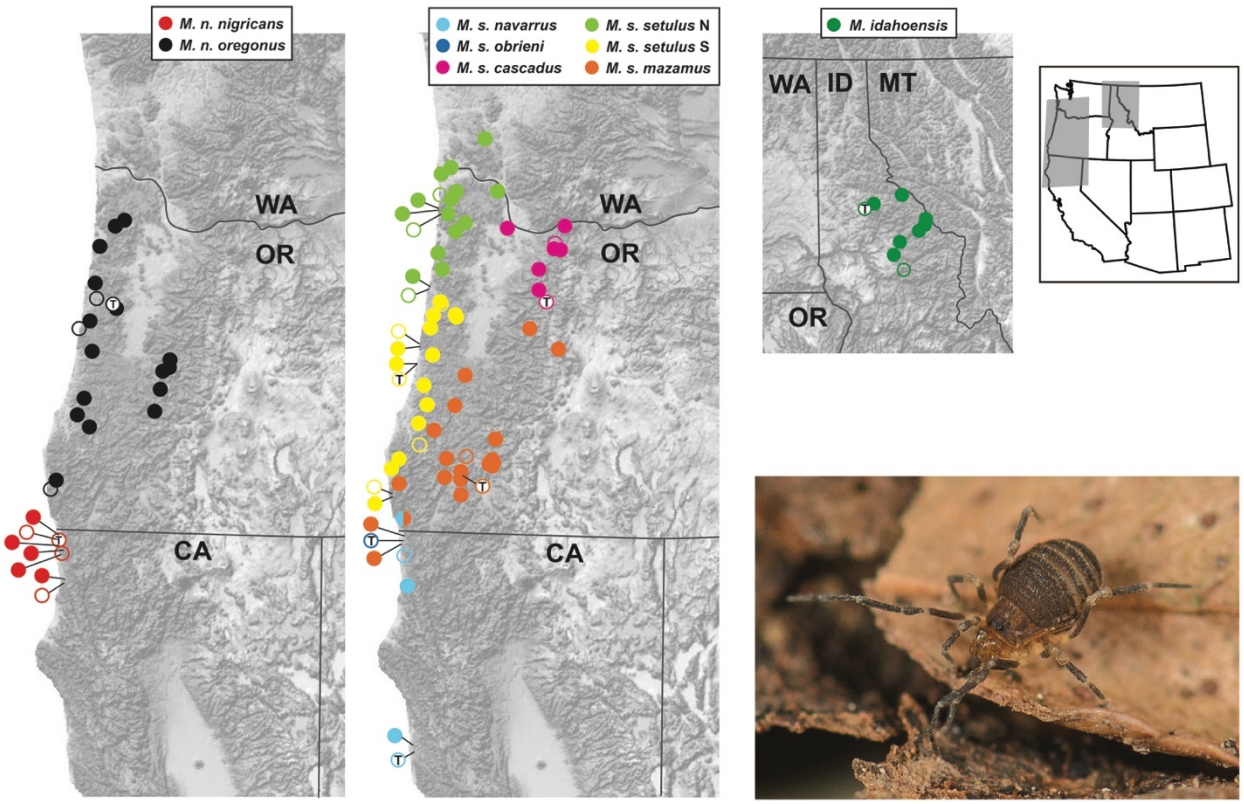

Figure 1. Geographic distribution of *Metanonychus*. Filled circles are collecting localities sampled for this study. Open circles are published records from Briggs (1971). Open circles with "T" indicate type localities. Live photo: *Metanonychus s. navarrus*.

Species Delimitation Workflow

We consider species as "separately evolving metapopulation lineages" (de Quieroz 2007), that in practice are genetic clusters of samples corresponding to monophyletic lineages that show fixed morphological differences. For the discovery phase, our a priori species are based on inferred well supported COI clades and fixed differences in male genitalic morphology. We use two popular discovery-based genetic clustering approaches as "standards" to assess the utility and results of three ML methods. All SNP-based clustering analyses utilized the

adegenet/STRUCTURE formatted file (.str) as input, which allowed minimal file format conversion from "standard" to ML approaches.

Species Discovery

The COI gene was sequenced for at least one sample from every collecting locality, plus two outgroups from the sister genus *Sclerobunus*, using multiple primer combinations (online Appendix 1). DNA was extracted using the Qiagen DNeasy kit (Qiagen, Valencia, CA) using 2-3 legs, PCR experiments followed Derkarabetian and Hedin (2014) and amplified fragments were Sanger sequenced at Macrogen USA. The Sanger-sequenced COI dataset was supplemented with COI sequences derived as "UCE-bycatch" (e.g., Zarza et al. 2017; Hedin et al. 2018) for all UCE samples (see below). COI sequences were manually aligned and a phylogeny was reconstructed using RAxML v.8 (Stamatakis 2014) with 500 bootstrap replicates and the GTRGAMMA model. COI divergence dating was conducted with BEAST 2.4.8 (Bouckaert et al. 2014) using two calibrations: a strict clock calibrated at 0.0178 (Papadopolou et al. 2010), and a date calibration for the outgroups *S. nondimorphicus* (from coastal Oregon/Washington) and *S. idahoensis* (from Idaho), a well-known biogeographic break typically dated to 2-5 MY (Brunsfeld et al. 2001, and references therein), which was set to a uniform distribution of (2, 5).

The male genitalia in harvestmen tend to be species-specific and have been used in systematic studies across all taxonomic levels since the mid-1900s. We examined male genitalia for multiple samples of all described species/subspecies using standard scanning electron microscopy techniques. Images were taken using the FEI Quanta 450 FEG environmental SEM at the San Diego State University Electron Microscope Facility.

Sequence Capture and SNPs

196 The number of studies utilizing UCEs in species delimitation and SNP-based population
197 level analyses are increasing (e.g., Smith et al. 2013; Blaimer et al. 2016; Harvey et al. 2016;
198 McCormack et al. 2016; Newman and Austin 2016; Zarza et al. 2016; Starrett et al. 2017; Hedin
199 et al. 2018). Extractions were conducted as above, except in most cases whole bodies were used
200 in digestions. Sequence capture of UCE loci followed the protocols available from the
201 ultraconserved.org website and as in Starrett et al. (2017) and Derkarabetian et al. (2018) using
202 the Arachnida 1.1Kv1 myBaits kit (Arbor Biosciences) designed by Faircloth (2017).
203 Sequencing was done at the Brigham Young University DNA Sequencing Center on a HiSeq
204 2500 with 125 bp paired-end reads.
205 Raw reads were processed using phyluce (Faircloth 2005), adapter removal and quality
206 control was done with an illumiprocessor wrapper (Faircloth 2013), and contigs were assembled
207 with Trinity version r2013-02-25 (Grabherr et al. 2011). When matching contigs to probes,
208 conservative values of 82 and 80 were used for minimum coverage and minimum identity,
209 respectively, to filter potential non-target contamination (Bossert and Danforth 2018). Loci were
210 aligned using MAFFT (Katoh and Standley 2013) and trimmed using gblocks (Castresana 2000;
211 Talavera and Castresana 2007) with settings --b1 0.5 --b2 0.5 --b3 10 --b4 4. All loci were
212 manually inspected in Geneious (Kearse et al. 2012) to fix obvious alignment errors and filtered
213 for obvious non-homologs. Contigs corresponding to COI were identified by a local BLAST
214 search in Geneious against available *Metanonychus* COI sequences. Although not used in species
215 delimitation, a concatenated matrix of UCE loci with 70% taxon coverage was used to
216 reconstruct a phylogeny using RAxML with 500 bootstraps and the GTRGAMMA model.
217 SNP datasets were created from sequence capture reads using published approaches (e.g.,
218 Zarza et al. 2017). The sample with the highest number of recovered UCE loci was used as a

reference genome (*M. idahoensis*, OP2432). After adapter removal and quality control, reads for all samples were aligned to the reference using bwa (Li and Durbin 2009), the resulting SAM files were sorted using samtools (Li et al. 2009), PCR duplicates were identified and removed using picard (http://broadinstitute.github.io/picard), and all BAM files were merged. The Genome Analysis Toolkit 3.2 (GATK; McKenna et al. 2010) was used to realign reads and remove indels and SNPs were then recalibrated using "best practices" (van der Auwera et al. 2013). After recalibration SNPs were called and vcftools (Danecek et al. 2011) was used to create SNP datasets which varied in the percent of taxon coverage needed to include a SNP (50% and 70%). One random SNP from each locus was selected and the script adegenet_from_vcf.py (github.com/mgharvey/seqcap_pop) was used to create STRUCTURE-formatted (.str) files.

Standard Genetic Clustering

As a comparison for the efficacy of unsupervised ML methods in inferring structure and optimal clustering, we used two popular approaches. First, STRUCTURE version 2.3.4 (Pritchard et al. 2000) was run for 1 million generations and 100,000 burnin on K values ranging from 2-10, with five replicates each. Structure Harvester (Earl and vonHoldt 2012) was used to determine optimal K via calculation of ΔK (Evanno et al. 2005) and Clumpak (Kopelman et al. 2015) was used to visualize output (http://clumpak.tau.ac.il/). Second, we used the adegenet R package (Jombart 2008; Jombart and Ahmed 2011) to conduct principal components analysis (PCA; dudi.pca function) and determine the optimal number of clusters and cluster assignment with discriminant analysis of principal components (DAPC) on scaled data.

Unsupervised ML Visualization

Three unsupervised ML approaches were used for clustering (see Table 1). We executed RF through the randomForest R package (Liaw and Wiener 2002), extracting the scaled data

242 from DAPC to a separate matrix. There are two important parameters associated with RF. The
243 ntree parameter, the number of classification trees to create, was set to 5000. The mtry, the
244 number of splits in the classification tree, was left at default for a classification analysis, which is
245 square root the number of variables. The resulting proximity matrix was then used in both classic
246 MDS (cMDS) and isotonic MDS (isoMDS). cMDS was executed using the MDSplot function in
247 the randomForest package and isotonic MDS was conducted using the isoMDS function in the
248 MASS R package (Venables and Ripley 2002).

249 VAE was implemented with a custom script utilizing the Keras python deep learning
250 library (https://keras.io; Chollet 2015) and the TensorFlow machine learning framework
251 (www.tensorflow.org; Abadi et al. 2015). As input for VAE we use SNP matrices converted via
252 "one-hot encoding" where each nucleotide is transformed into four binary variables unique to
253 each nucleotide (e.g., A = 1,0,0,0; C = 0,1,0,0; etc.) including ambiguities (e.g., M = 0.5,0.5,0,0)
254 using a custom script. The VAE is composed of an encoder and a decoder. The encoder takes the
255 one-hot encoded SNP data and infers the distribution of latent variables, given as a normal
256 distribution with a mean (μ) and standard deviation (σ). The decoder then maps the latent
257 distribution to a reconstruction of the one-hot encoded SNP data. As there are two latent
258 variables, SNP data for each sample can be visualized as a reduced two-dimensional
259 representation. Details of the VAE and the training procedure are in Supplementary File: Figure
260 1.

261 t-SNE was executed using the R package tsne (Donaldson 2016). After preliminary
262 testing, several parameters were specified: maximum iterations (max_iter=5000), perplexity=5,
263 initial dimensions (initial_dims=5), and number of dimensions for the resulting embedding
264 (k=2). The maximum iterations value is relatively straightforward to determine as the KL

265 divergence (a measure of the difference between high and low dimensional representations)
266 should stabilize at a minimum. Perplexity is a measure of the balance between the local and
267 global elements of the data; essentially how many neighbors a particular sample can have. This is
268 a somewhat subjective parameter, where lower perplexity will produce tight well separated
269 clusters, and higher values will produce more diffuse less distinguishable clusters. However,
270 results and clusters are typically robust across a wide range of perplexity values (Pedregosa et al.
271 2011) and methods have been introduced to make perplexity selection automatic (Cao and Wang
272 2017). With large datasets it is recommended to perform dimensionality reduction on the data via
273 PCA or a similar algorithm prior to implementing t-SNE (Pedregosa et al. 2011). As such, we
274 perform t-SNE using the results of the initial PCA as input.

275 With RF and t-SNE, we also tested three different types of input format using the 70%
276 SNP dataset. First, the SNPs were represented as raw nucleotides with ambiguities in standard
277 IUPAC coding, extracted directly from .vcf files using the vcf2phylip script
278 (github.com/edgardomortiz/vcf2phylip). Second, the raw SNPs were converted to haplotypes
279 using the script SNPtoAFSready.py (github.com/jordansatler/SNPtoAFS). Third, the raw
280 unphased nucleotides were converted into numerical format via one-hot encoding. For the first
281 two datasets, the Ns were coded as blank, and PCA could not be conducted as the variables are
282 categorical. As such, t-SNE was run using the cMDS output.

283 *Unsupervised ML Clustering*

284 To assess the performance of clustering based on ML results relative to widely used
285 STRUCTURE and DAPC approaches, four sets of clustering analyses were conducted using RF,
286 VAE, and t-SNE outputs. First, to confirm that cluster assignments are equivalent to DAPC and
287 STRUCTURE assignments, PAM clustering was conducted using the cluster R package

(Maechler et al. 2018) with the optimal K selected from DAPC. The next three clustering methods test whether the optimal K can be inferred correctly relying solely on unsupervised ML results. PAM clustering was done on all output, including both the proximity matrix and cMDS for RF, across K of 2-10 with the optimal K having the highest average silhouette width (Rousseeuw 1987). Next, PAM clustering was conducted with the optimal K determined via the gap statistic using k-means clustering implemented in the factoextra R package (Kassambara and Mundt 2017). Finally, optimal K and clusters were determined via hierarchical clustering with the mclust R package (Scrucca et al. 2017) using only components retained via the broken stick algorithm implemented in the PCDimension R package (Coombes and Wang 2018).

Species validation

We implement the commonly used Bayes Factor delimitation approach (*BFD; Leaché et al. 2014) with SNAPP (Bryant et al. 2012) using a 70% UCE SNP matrix created by the phyluce script "phyluce_snp_convert_vcf_to_snapp". Multiple species hypotheses were tested based on current taxonomy, a priori species, ML clustering results, and an analysis where each individual specimen was treated as a unique species. SNAPP analyses were run with default settings for 100,000 generations, 10,000 burnin, and 48 steps. Each analysis was run twice to ensure consistency. Bayes Factors (Kass and Raftery 1995) were calculated (2 * log likelihood difference) to determine relative support of species hypotheses.

Next, we use the RF-based program CLADES (Pei et al. 2018), which uses Support Vector Machines, a type of supervised ML, to build a classifier based on labeled samples where samples are classified as either the same or different species. Several population genetic statistics are calculated for the simulated training data and the observed data, which are then treated as variables. The classifier is then used to infer whether the observed a priori species are equivalent

311 to the same or different species. As input we use the UCE loci in two different analyses: 1) an
312 analysis validating a priori species hypotheses ("spp" dataset); and 2) an analysis in which every
313 individual was treated as a distinct species ("ind" dataset).

314 *Published Datasets*

315 Uma notata *complex*. – Gottscho et al. (2017) explored lineage diversification and species
316 limits in fringe-toed lizards of the *Uma notata* species complex, a group with a complicated
317 taxonomic history. Using ddRAD data they find significant levels of gene flow between multiple
318 species and determine that *U. rufopunctata* is a hybrid population. Several genetic clustering
319 algorithms were used with differing results: DAPC favored an optimal K=5 (grouping the hybrid
320 *U. rufopunctata* with *U. cowlesi*), while a model with admixture favored an optimal K=6
321 (splitting *U. scoparia* and showing varying levels of admixture for *U. rufopunctata* samples
322 between *U. cowlesi* and *U. notata*). We reanalyzed their data with the intention of assessing
323 unsupervised ML clustering/visualization in the face of significant gene flow and known hybrids.
324 The published dataset with 597 SNPs was downloaded from Dryad
325 (https://doi.org/10.5061/dryad.8br5c).

326 Phrynosoma coronatum *complex*. – The coast horned lizards of the genus *Phrynosoma*
327 *coronatum* complex have received much attention with many species hypotheses put forth
328 (summarized in Leaché et al. 2018). In an integrative approach Leaché et al. (2009) recover five
329 well supported mtDNA clades that show little concordance with nuclear loci, ultimately
330 integrating ecology and morphology to support three species (*P. blainvillii*, *P. cerroense*, and *P.*
331 *coronatum*). More recently, Leaché et al. (2018) use SNP data coupled with *BFD testing all
332 hypotheses derived from previous research, ranging from one to six species. A five species
333 model is given the highest support, reflecting mtDNA and splitting *P. blainvillii* into three

groups. Here, we use unsupervised ML methods for clustering, but more importantly to demonstrate their utility as a data visualization tool in a dataset showing high uncertainty in cluster probability assignments (fig. 1 of Leaché et al. 2018). Data were downloaded from dryad (https://doi.org/10.5061/dryad.k7k4m), and the SNP dataset in the .xml file was manually extracted and converted to .csv format for import into R.

RESULTS

Species Discovery

Metanonychus specimens were collected from 79 different collecting localities. A total of 117 sequences were included in COI analyses (alignment length of 1182 bp); all new COI sequences have been deposited to GenBank (XXXX -XXXX). Seventy-seven sequences were acquired via Sanger sequencing and 38 were sequenced as UCE bycatch, with five samples being sequenced by both approaches, for a total of 110 *Metanonychus* specimens (plus two outgroups). UCE bycatch sequences possessed no stop codons, and for those samples sequenced via Sanger and as UCE bycatch, sequences were identical. COI divergence dating supports the ancient origin of this genus dating to ~25 Ma (Supplementary File: Fig. 2). The RAxML phylogeny recovers a deep split between the "*nigricans* group" containing both subspecies of *M. nigricans* and the "*setulus* group" containing *M. idahoensis* and *M. setulus* with all subspecies. Each currently named taxon is monophyletic with bootstrap support values of 100 (Supplementary File: Fig. 3), except the *setulus* subspecies is polyphyletic separated into geographically cohesive northern and southern clades, although support for relevant internal nodes are weak.

Male genitalic morphology show clear differences between all species/subspecies, including northern and southern clades of the *setulus* subspecies (Supplementary File: Fig. 4).

356 Taken together, the discovery phase identified eight a priori species corresponding to the
357 currently named species/subspecies (except *obrieni,* Appendix 1) with the *setulus* subspecies
358 split into two genetically divergent, geographically cohesive clades with fixed differences in
359 genitalic morphology.

360 *Sequence Capture and SNPs*

361 A total of 38 *Metanonychus* samples were included in UCE analyses, 36 of which were
362 newly sequenced (online Appendix 1). Raw reads for sequence capture data have been deposited
363 to SRA (XXXX). The 70% matrix included 185 loci (average of 158 per sample) with a mean
364 locus length of 411 bp and a total length of 75,944 bp. The UCE phylogeny similarly confirms
365 the monophyly of the *nigricans* and *setulus* groups and recovered the same clades as COI, but all
366 internal nodes were fully supported (Supplementary File: Fig. 3). The *setulus* subspecies is
367 recovered as monophyletic, albeit with reciprocally monophyletic northern and southern
368 lineages. A 50% UCE matrix (278 loci, mean locus length of 384 bp, total length of 106,786 bp),
369 produced an identical topology (not shown).

370 Due to the relatively high levels of divergence in *Metanonychus*, preliminary exploration
371 of SNP datasets including all 38 samples resulted in datasets with too few loci or too sparse a
372 matrix, with *M. nigricans* samples missing an average of ~60% of SNPs (~11% average samples
373 in the *setulus* group). For the purposes of demonstrating ML clustering in *Metanonychus*, we
374 focus on the monophyletic *setulus* group with six a priori species identified in the discovery
375 phase. The *setulus* group included 30 samples and the 70% SNP dataset contained 316 SNPs
376 (average of 250 per sample), while the 50% dataset contained 1263 SNPs (average of 774 per
377 sample).

378 *Standard Genetic Clustering*

379 For the 70% and 50% SNP datasets, both STRUCTURE (ΔK) and DAPC favored an
380 optimal K=6 (Fig. 2 a, b; Fig. 3; Supplementary File: Fig. 5 and Fig. 6), recovering all six a
381 priori *setulus* group species as distinct clusters, including the separate clades of the *setulus*
382 subspecies.

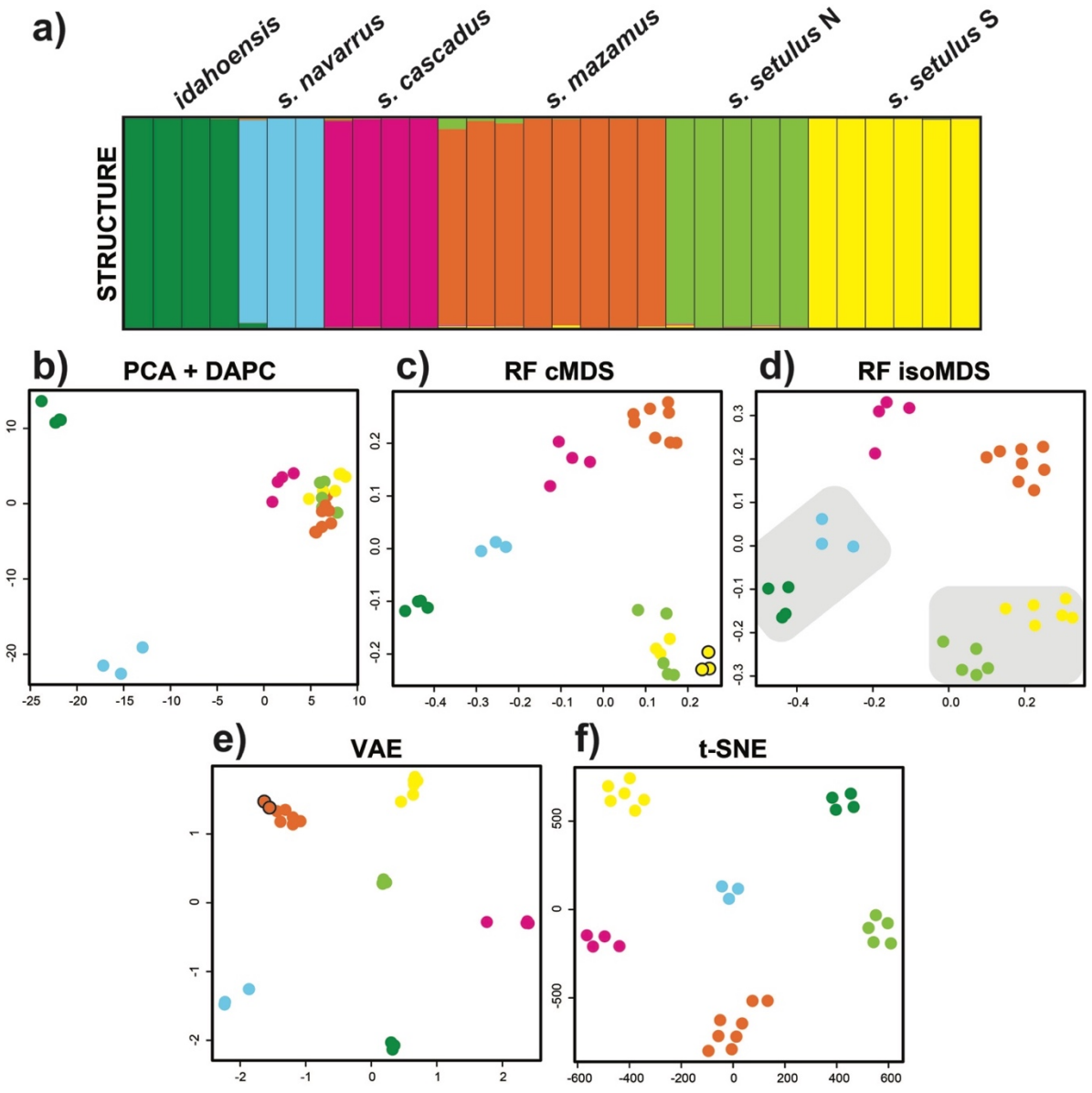

383

384 **Figure 2**. Clustering results for the *Metanonychus* 70% SNP dataset. a) STRUCTURE plot. b) PCA plot with DAPC
385 clusters. c) random forest cMDS plot, all clustering algorithms favored K=6, except hierarchical clustering with K=7
386 (seventh cluster indicated with black outline). d) random forest isoMDS plot, all clustering algorithms favored K=6,
387 except PAM clustering of RF output with K=4 (lumped clusters are indicated with grey shading). e) VAE plot, all
388 clustering algorithms favored K=6, except hierarchical clustering with K=7 (seventh cluster indicated with black

389 outline). f) t-SNE plot, all clustering algorithms favored K=6. cMDS = classic multidimensional scaling, isoMDS =
390 isotonic multidimensional scaling.

391 *Unsupervised ML*

392 Unsupervised ML analyses were relatively quick and computationally inexpensive taking
393 1-3 minutes for each of the three algorithms when run locally. All ML analyses were run
394 multiple times producing identical clustering results. For the 70% dataset, all clustering
395 approaches for RF (cMDS and isoMDS), VAE, and t-SNE resulted in an optimal of K=6, with
396 the exception of the cMDS with hierarchical clustering resulting in an optimal of K=7 splitting
397 the southern clade of the *setulus* subspecies, and hierarchical clustering of VAE with an optimal
398 of K=7 splitting *mazamus* (Fig. 2, Fig. 3). Importantly, all K=6 clustering assignments were
399 identical to those from DAPC and STRUCTURE. For the 50% dataset, an optimal of K=6 was
400 found for the majority of analyses (Supplementary File: Fig. 5 and Fig. 6). However, the cMDS
401 using hierarchical clustering resulted in K=7, splitting the northern clade of the *setulus*
402 subspecies, and hierarchical clustering of VAE resulted in K=7, splitting *mazamus*. Clustering of
403 the 50% dataset based on isoMDS was more variable, with an optimal K=4 for hierarchical
404 clustering and K=1 for the gap statistic. All VAE and t-SNE clusters were obvious. VAE clusters
405 were robust, being recovered identically across five replicate analyses, and clear separation
406 between clusters is seen when σ (standard deviation) is included (Supplementary File: Fig. 7). t-
407 SNE clusters were robust to perplexity values from 5-25, after which samples became randomly
408 dispersed (Supplementary File: Fig. 8). The unsupervised ML approaches produced plots with
409 easier interpretability relative to PCA, with species clusters showing more separation in two-
410 dimensional space. Similar plots for RF and t-SNE were obtained using input where SNPs were
411 coded in multiple ways (Supplementary File: Fig. 9).

412

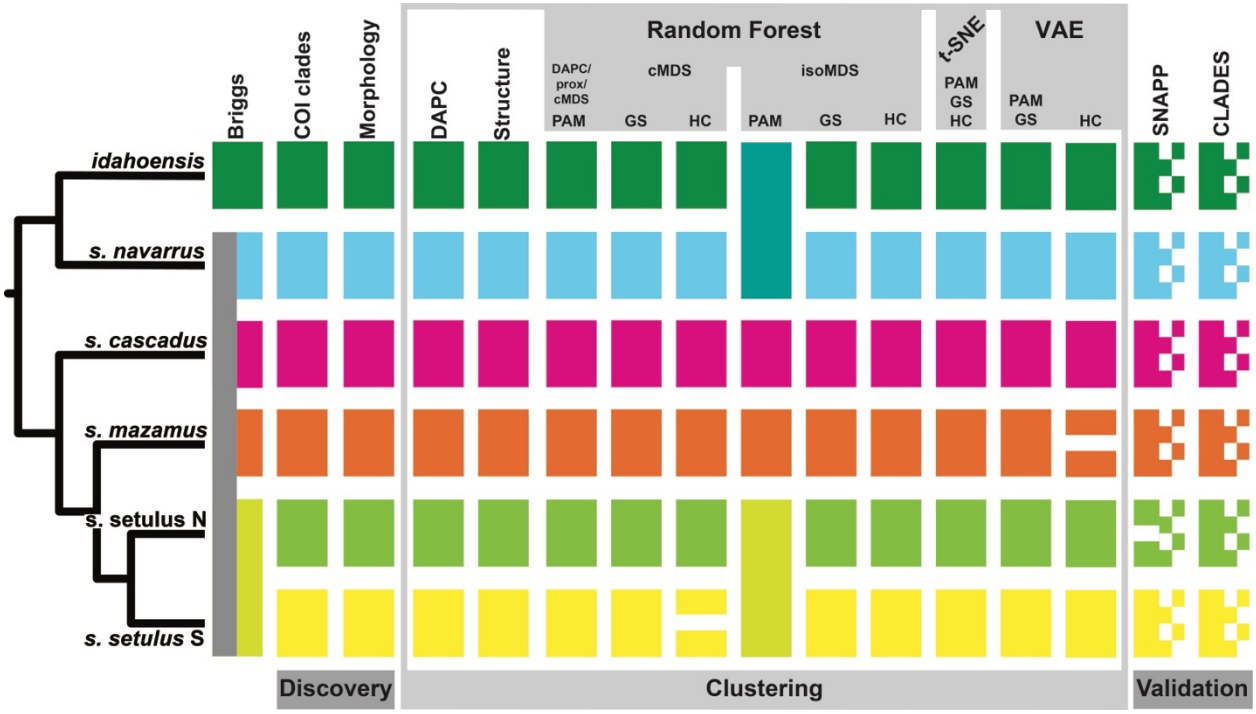

413

414 **Figure 3.** Integrative species delimitation results for the *Metanonychus* 70% SNP dataset. Species tree at left
415 adapted from RAxML analysis of 70% UCE dataset. GS = gap statistic, HC = hierarchical clustering.

416 *Species Validation*

417 *BFD showed increasing likelihood with increasing species (Table 2), with Bayes
418 Factors heavily favoring the analysis in which all individual specimens were treated as distinct
419 species (K=30). Only considering hypotheses recovered in the discovery phase, the "7N" species
420 hypothesis was favored, recognizing all six a priori species plus two species in the northern clade
421 of the *setulus* subspecies. CLADES requires that each locus have data for at least one sample
422 within every a priori species. As a result, the "spp" dataset had 177 loci and the "ind" dataset had
423 12 loci. CLADES supported the species status of all six a priori species. However, species status
424 was also supported when each sample was treated as a distinct species (Fig. 3).

425 **Table 2.** Results of *BFD hypothesis testing.

Species	Justification	A	B	Bayes Factor
2	Briggs' species	-3674.33	-3885.74	~6924
4	70% isoMDS PAM, 50% isoMDS HC	-2917.94	-2910.14	~5192
5	Briggs' species + subspecies	-2384.94	-2386.83	~4135
6	a priori species	-2210.48	-2211.17	~3785
7 M	split *s. mazamus*: VAE HC	-2135.1	-2136.23	~3635
7 N	split *s setulus* N: 50% cMDS HC	-1797.95	-1798.71	~2960
7 S	split *s. setulus* S: 70% cMDS HC	-2165.62	-2166.25	~3695
30	all individuals	-320.3	-316.24	-

426

427 *Supplementary Material*

428 All *Metanonychus* input matrices (COI, UCE SNPs, UCE loci, and .csv files) are
429 available from the Dryad Digital Repository: http://dx.doi.org/10.5061/dryad.[NNNN]. Resulting
430 phylogenies are available via TreeBASE (XXXX). Two custom scripts were created to run ML
431 analyses: an R script to run random forest, t-SNE, and all clustering algorithms
432 (github.com/shahanderkarabetian/uml_species_delim), and a python script to run VAE
433 (github.com/sokrypton/sp_deli).

434 *Published Datasets*

435 Uma notata *complex*. – All clustering based on RF with cMDS favored a K=5 scenario,
436 with cluster assignment identical to DAPC results, with the exception of hierarchical clustering
437 favoring an optimal K=6 (Fig. 4). In this case, a distinct cluster was identified for all *U.*
438 *rufopunctata* and two samples of *U. notata*. The optimal of K=6 recovered in Gottscho et al.
439 (2017) does not differentiate *U. rufopunctata*, instead splitting *U. scoparia*. The cMDS plots do
440 show two somewhat distinct samples of *U. scoparia*, which correspond to samples placed in the
441 sixth cluster. Clustering results ranged from K=4 in PAM, lumping *U. cowlesi*, *U. notata*, and *U.*

442 *rufopunctata*, to K=7 in some replicates of t-SNE clustered with gap statistic splitting *U.*
443 *scoparius*. The t-SNE and VAE plots recover the hybrid species *U. rufopunctata* as a linear
444 "grade" between the parental species *U. cowlesi* and *U. notata*, and assignment uncertainty of the
445 hybrid samples are seen when σ is also visualized (Supplementary File: Fig. 7).

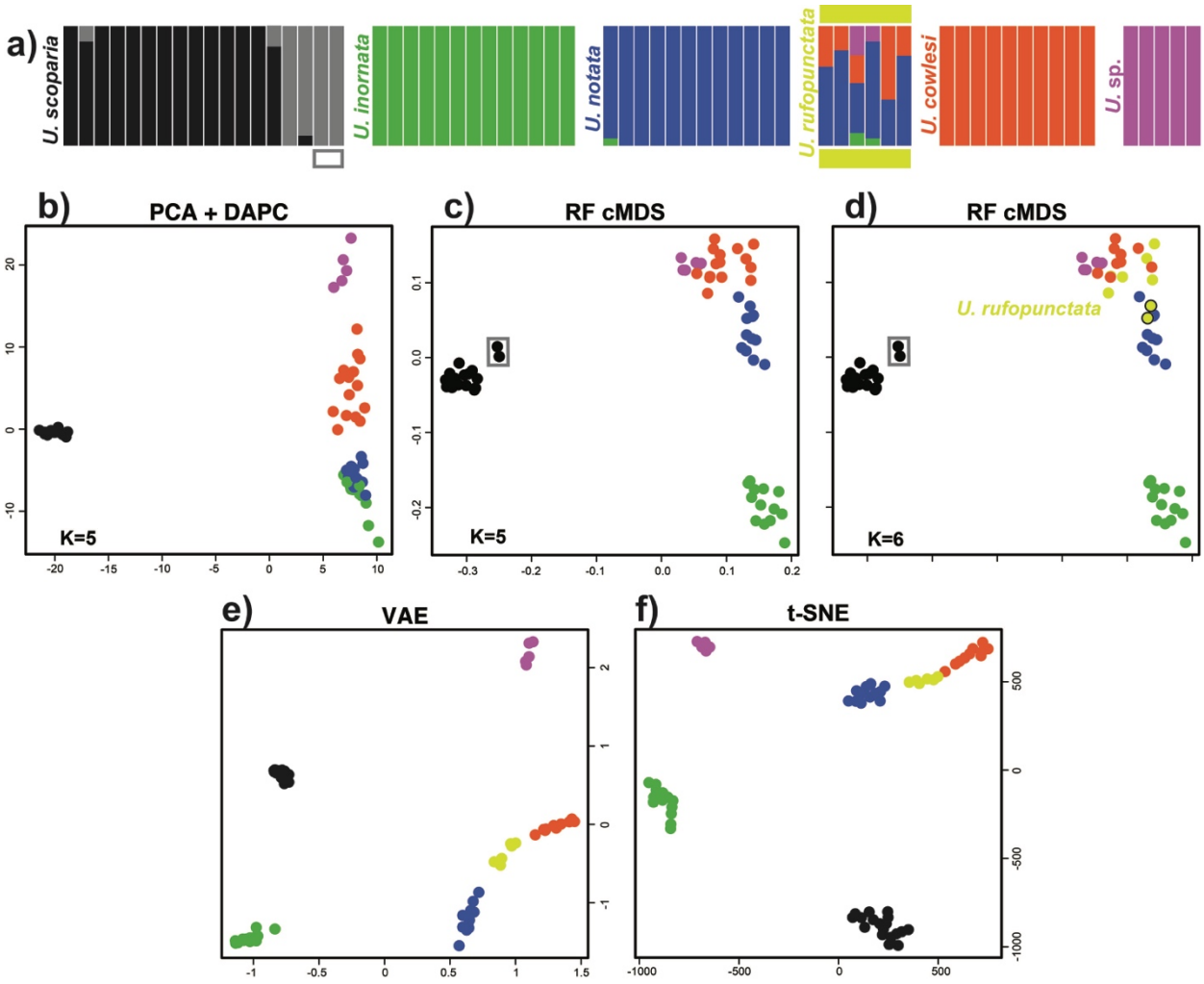

446

447 **Figure 4.** Clustering results for *Uma* dataset. a) STRUCTURE plot adapted from Gottscho et al. (2017). b) PCA
448 with DAPC clusters. c) random forest cMDS plot with clusters identified via DAPC, PAM, and gap statistic. d)
449 random forest cMDS plot with clusters identified via hierarchical clustering. e) VAE plot with K=6 a priori species.
450 f) t-SNE plot with K=6 a priori species. Species are color coded as in Gottscho et al. (2017). Note: algorithmic
451 clustering was only conducted on random forest output.

452 Phrynosoma coronatum *complex.* – As expected, clustering via DAPC, RF, VAE, and t-
453 SNE with nuclear SNP data did produce groups congruent with mitochondrial clades, with the
454 exception of *P. coronatum* (Fig. 5). DAPC favored K=4 (*P. coronatum*, southern *P. cerroense*,

455 northern CA *P. blainvillii*, and northern P. *cerroense* + the rest of *P. blainvillii*), while PAM
456 clustering favored K=2. The differing cluster assignments of *P. cerroense* lineages reflects their
457 polyphyly in the SNP phylogeny of Leaché et al. (2018). While all plots arrange samples in a
458 way reflective of their genetic similarity, the more diffuse spatial arrangement of samples in the
459 t-SNE embedding and the σ of the VAE are particularly informative and reflective of cluster
460 probability assignments for *P. blainvillii* samples (Fig. 5d and Supplementary File: Fig. 7).

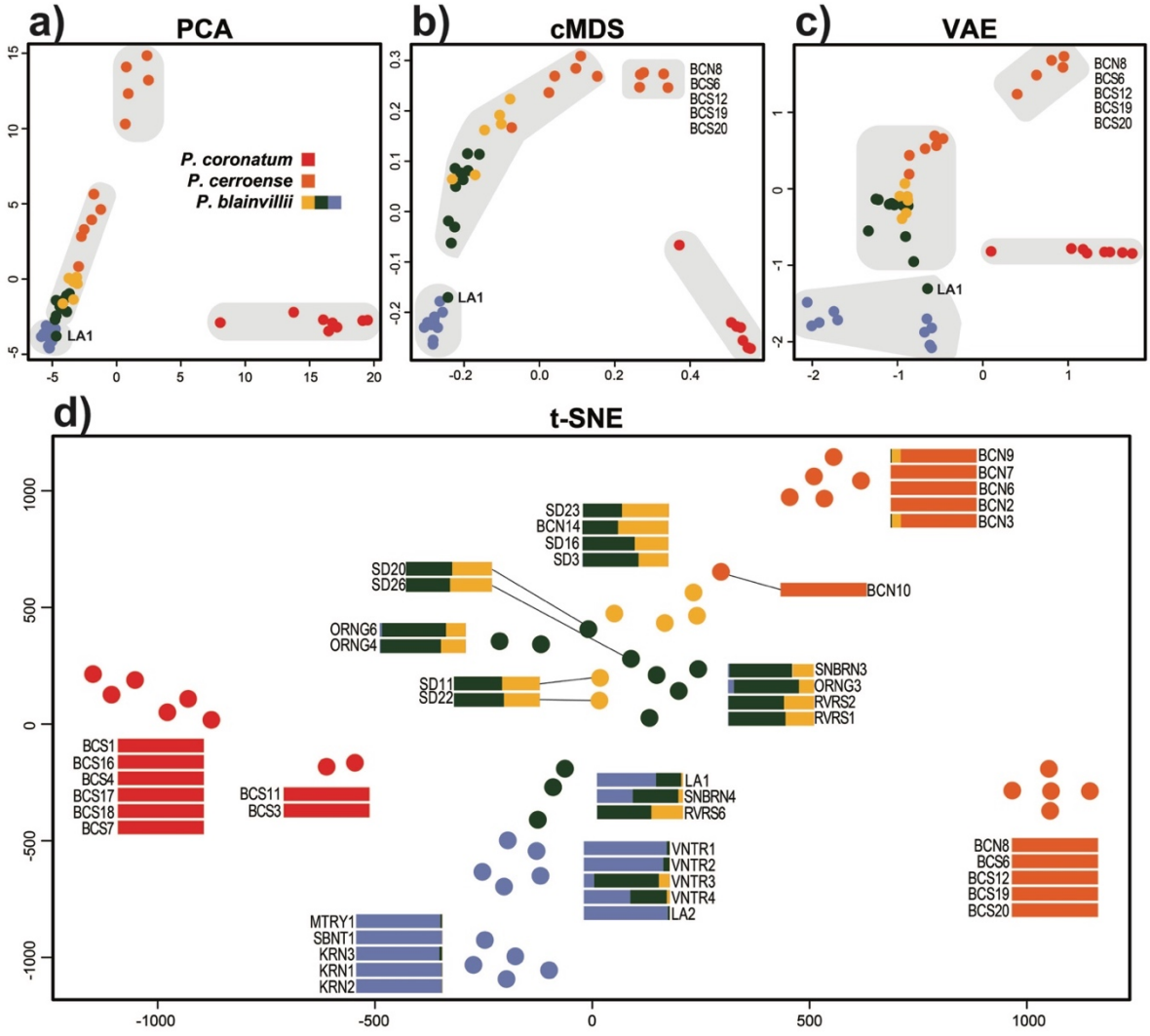

461

462 **Figure 5.** Clustering results for *Phrynosoma* dataset. a) PCA plot. b) random forest cMDS plot. c) VAE plot. For
463 parts a-c) samples are colored by mtDNA clades recovered in Leaché et al. (2009), and grey boxes indicate optimal
464 clustering of K=4 recovered via DAPC. d) t-SNE embedding, with corresponding assignment uncertainty for each
465 sample adapted from Leaché et al. (2018). Samples are color coded as in Leaché et al. (2018).

DISCUSSION

Reconsidering (SRE) Species Delimitation

Commonly used validation approaches relying on genomic-scale data have the potential to identify population structure and oversplit taxa (e.g., Sukumaran and Knowles 2017), a problem that can be exacerbated when studying SRE taxa with inherently high levels of population structure. Model-based validation analyses relying on the multispecies coalescent as currently implemented (e.g., BPP, SNAPP) seek to identify separate panmictic gene pools. This approach may not be suitable for *all* taxa given the diversity of biological characteristics unique to particular groups or organismal types with differing degrees of population structure and isolation, etc. (Sukumaran and Knowles 2017). While the issue of population structure in species delimitation has recently come under focus from a methodological perspective, the potential misinterpretation of population structure as species level divergences in empirical data has been a concern for taxonomists focusing on SRE taxa for a relatively long time (e.g., Hedin 1997), and continues to be so (e.g., Boyer et al. 2007; Bond and Stockman 2008; Niemiller et al. 2012; Barley et al. 2013; Satler et al. 2013; Fernández and Giribet 2014; Hedin 2015; Hedin et al. 2015).

Unsupervised ML clustering of SNP data provided reasonable species hypotheses that were largely identical to commonly used discovery-based analyses. However, when used with validation methods, the same data supported unrealistic results severely overestimating the number of species. Most importantly, clusters identified in unsupervised ML approaches obviously correspond to species, implying that cluster separation was dominated by species-level divergences and not population structure. If validation analyses show increasing support for more complex species delimitation models, up to the most unrealistically complex model

possible given the data (i.e., each individual specimen as a distinct species), those analyses do not contribute useful information to the final species hypotheses. Similarly, the possibility of the most complex model being favored, whether actually tested or not, makes "support" for any less complex alternative models meaningless. If we did not run the K=30 SNAPP analysis or the "ind" analysis in CLADES, a more realistic 6-7 species hypothesis would be favored validating all a priori species, without any consideration of more complex hypotheses that are actually more likely. For *Metanonychus*, validation analyses were effectively ignored in the formation of final species hypotheses, and the information content of the SNP dataset was squandered, not being used to its full potential. While *BFD/SNAPP is useful for testing alternative assignment hypotheses, its use as a validation tool to determine the number of species is certainly problematic for SRE taxa, and more broadly for any taxon with significant population structure.

Because model-based validation analyses have the potential to delimit population level divergences, that does not mean they *only* identify population-level divergences. However, the confirmation that validation analyses are operating at the species level can only be assessed when species delimitation is conducted in an integrative framework, and we reiterate the statement by Sukumaran and Knowles (2017) that external information (i.e., different data types) are needed to confirm delimitations made based on genetic-only analyses. Ultimately, we argue that the separation of empirical species delimitation into two distinct phases (discovery and validation) limits the potential utility of the "validation" data type in informing species hypotheses in a truly integrative manner. Data types used in the discovery phase inform the a priori species hypotheses used as input for the validation phase, but the data type used in validation does not reciprocally inform the other data types. Ideal integrative taxonomy as described by Schlick-Steiner et al.

511 (2010) utilizes multiple data types in a reciprocally illuminating framework where discordance
512 between datasets requires consideration of the underlying biological processes.

513 *Machine Learning in Species Delimitation*

514 The goal of this study was to explore how well unsupervised ML methods can
515 successfully identify clusters equivalent to species and correctly infer the expected number of
516 clusters. We argue that species delimitation in *Metanonychus* was relatively "simple" showing
517 essentially no discordance between datasets and provided an excellent study system to explore
518 novel approaches. In an integrative framework, our results suggest that the expected number of
519 species, determined via mitochondrial and morphological analyses, can be correctly inferred
520 across multiple clustering algorithms using the RF distances, the latent variables of VAE, and the
521 t-SNE embeddings. Most importantly, unsupervised ML approaches coupled with standard
522 clustering algorithms did not oversplit the data by distinguishing samples based on population-
523 level structure, but instead formed clear clusters equivalent to species-level divergences. While
524 these unsupervised approaches seemingly work well with relatively clear species, their ability to
525 correctly cluster samples in more difficult speciation scenarios (e.g., rapid and recent divergence,
526 divergence with gene flow, etc.) remains to be tested, although results in *Uma* are promising.
527 For unsupervised RF, more consistent and "accurate" clustering was achieved using the
528 cMDS output. Like DAPC, multiple dimensions are used to inform the optimal clustering
529 strategy. Conversely, isoMDS by default only outputs two dimensions for clustering. isoMDS
530 may be suitable for significantly diverged taxa, in which case it can sometimes produce a better
531 two-dimensional visualization of the data relative to cMDS. VAE and t-SNE clusters were
532 exceedingly obvious regardless of data type, and robust across multiple iterations and varying
533 parameters. t-SNE was designed purely for the visualization of high dimensional data, although

given a low dimensional embedding as output, clustering is an obvious application. It has been noted that t-SNE clusters, cluster size, and distances between clusters may not have any relevant meaning (Wattenberg et al. 2016) and clusters should be interpreted with caution. As t-SNE does not preserve the density of actual clusters completely, density-based clustering algorithms (Ester et al. 1996; Campello et al. 2013) may offer an improvement relative to other clustering approaches. Regardless, in the datasets used here, inferred clusters have obvious biological meaning corresponding to species which were corroborated by other analyses and data types. More consistent and accurate clustering results were obtained with the 70% taxon coverage dataset. Samples with a higher percentage of missing data might be reconstructed in closer proximity by unsupervised ML methods, regardless of phylogenetic proximity, simply because they share high levels of missing data. This is particularly the case with data converted to one-hot format where a missing SNP was coded as "0,0,0,0", although we designed our VAE to mask missing data.

Neural networks have mostly been designed/used for identifying the latent space of images, the most relevant examples including the citizen science natural history observational platform iNaturalist (www.inaturalist.org) and classification of ants (Boer and Vos 2018). Here we show that VAEs, which leverage neural networks to learn a probability distribution of the data, can learn phylogenetic structure with the latent variables. In contrast to t-SNE, VAEs are nicely derived from formal Bayesian probability theory, and can hence be used to score the probability that the new data belongs to a trained set of data or is a new species. The standard deviation around samples/clusters is an inherent result of a VAE analysis and visualization makes the assessment of cluster distinctiveness or uncertainty relatively straightforward. One drawback is that it is not straightforward when to stop training a VAE. Overtraining a VAE can

lead to overfitting the data, which results in clusters that are still present, but the probability distribution over the data is less general, and hence cannot be used reliably for downstream analysis. One solution is to partition a small fraction of the training data as a validation set, which can be used to determine when training should be stopped, a technique in ML known as early stopping (Goodfellow et al. 2016), although we use a "dropout" approach to prevent overfitting. Given results presented here, the robustness of output to parameter variation, and its Bayesian nature, VAEs are very promising for future incorporation into systematic applications.

Data visualization is an important aspect of empirical research. With genetic data, whether used as loci or SNPs, this can be in the form of a phylogeny or via a dimensionality reduction method. Regardless of whether downstream clustering is performed, unsupervised ML methods like t-SNE and VAE offer excellent options for relatively quick and informative data visualization that can help examine uncertainty in a priori groupings or recognize misidentifications and paraphyly, both of which are problematic for species hypotheses if data are destined for downstream model-based analyses. The placement of hybrid populations of *Uma* and the arrangement of assignment uncertainty in *Phrynosoma* are displayed in low-dimensional space in spatially meaningful ways. The recently developed Uniform Manifold Approximation and Projection method (McInnes and Healy 2018) is a dimensionality reduction technique similar to t-SNE but with numerous benefits including better preservation of global structure and potential embedding in larger dimensional space benefitting downstream clustering.

Unsupervised ML methods do not make assumptions about data type (e.g., genetic versus morphological, etc.); data are merely treated as data. If approaches that are not specifically designed for a particular data type successfully identify/corroborate a priori species, the resulting species decisions are more robust. However, the underlying assumption is that the analyses are

operating at the species level. As with many dimensionality reduction techniques, unsupervised ML methods will uncover any underlying structure regardless of the taxonomic level or type of data. As such, integrative taxonomy with multiple data types and analytical approaches is ideal. Conversely, this insensitivity to taxonomic scale makes unsupervised ML relevant to population level analyses and phylogeography as well as species delimitation in taxa across varying divergence times, for example, divergences of ~20 Ma in the *Metanonychus setulus* group down to much more recent species divergences of <1 Ma reported for *Uma* (Gottscho et al. 2017).

An additional appeal of some ML approaches is their ability to be conducted in a "semi-supervised" manner, where some samples can be labeled (e.g., assigned to a species) while others are left unassigned. For example, semi-supervised analyses could be used for species assignment of samples with unknown determination, like females of *Metanonychus*, or in taxa where the vast majority of specimens are known from juveniles that cannot be identified to species (e.g., Hedin et al. 2018). While fully supervised approaches have been used for this same reason, for example with COI barcoding (e.g., Weitschek et al. 2014; Archer et al. 2017), utilizing a semi-supervised ML approach (e.g., McInnes and Healy 2018) saves the need for creating a training dataset and associated assumptions. In either case, given the increasing incorporation of museum specimens in genomic analyses (McCormack et al. 2016; Blaimer et al. 2016; Ruane and Austin 2017; Sproul and Maddison 2017) it is now feasible to directly include type specimens in species delimitation. In the case of semi-supervised methods, type specimens (or specimens from type localities, etc.) can be included in analyses as labeled data while all other samples are left unlabeled, or in a supervised approach, data from type specimens could be used in training dataset construction.

602 If model testing is integral to the study it seems more logical, particularly in cases where
603 genetic data is the only reliable way to assess species limits (i.e., cryptic species), to rely on
604 algorithms that utilize prior information in the form of training data based on parameters
605 associated with the particular biological characteristics of a given organismal type, thus taking
606 the biology of the organism more directly into account. For potential future analyses of SRE
607 harvestmen using supervised ML methods, training data could consist of multiple "curated" SRE
608 datasets where species are known and well-supported, which would then be used for SRE taxa
609 with unknown or uncertain numbers of species. While CLADES oversplit *Metanonychus*
610 supporting every individual as a species, we do not see this as a negative for the approach, but
611 rather as imperative to create and use curated training datasets reflecting the biological
612 characteristics of the study organism to fully leverage the power of this approach. More recently,
613 Smith and Carstens (2018) developed delimitR, a supervised ML approach that treats species
614 delimitation as a classification problem, using the binned multidimensional Site Frequency
615 Spectrum as the predictor variable to build an RF classifier that can distinguish among different
616 speciation models, the response variables, selecting the model with the most votes. Training data
617 is simulated based on specification of several priors (guide tree, population size, divergence time,
618 migration) either known or estimated for the particular study system. DelimitR is a promising
619 approach as priors are used to create the simulated data for classifier construction, making the
620 analysis more specific to the biology of the focal taxon.
621 In general, unsupervised ML approaches offer the benefits of better data visualization in
622 two-dimensional space and the ability to accommodate various data types. Like current methods
623 combining multiple data types into a single analysis (e.g., Guillot et al. 2012; Solis-Lemus et al.
624 2015), it may be feasible to do an integrative unsupervised ML analysis where various data types

(e.g., morphological, genetic, chemical profiles, etc.) are combined into a single dataset for downstream clustering. Many ML algorithms are well-suited for species delimitation, providing promising avenues of incorporation into standard systematics protocols and excellent resources are available for implementation (e.g., http://scikit-learn.org, https://keras.io, www.tensorflow.org). ML algorithms, even those designed for image analysis or pattern and text recognition, all seek to identify and learn the underlying structure of input data via dimensionality reduction of some form. This can be leveraged for all data types in diverse ways, for example, representing a multidimensional vector of population genetic statistics as an image to be analyzed via neural networks (Kern and Schrider 2018). As recently discussed in regard to population genetics (Schrider and Kern 2018), with a basic understanding of the types of ML algorithms, the applications to species delimitation become obvious and exciting with the potential to aid in all aspects of systematic biology.

Learning from Metanonychus

Multiple data types and analytical approaches favor six species in the *setulus* group, providing robust final species hypotheses. Although some analyses favored more than six species, we prefer more conservative species hypotheses that are robust to data and analysis type (e.g., Carstens et al. 2013). As a result of integrative species delimitation, we elevate all subspecies of the *setulus* group to full species, now consisting of *M. idahoensis*, *M. navarrus* **new comb.**, *M. cascadus* **new comb.**, *M. mazamus* **new comb.**, and *M. setulus*. In addition, all analyses supported the northern clade of the *setulus* subspecies as a distinct species, which we describe as ***M. xxxx* n. sp.** Derkarabetian and Hedin (Appendix 1). Based on examination of type specimens, *M. obrieni* is synonomized with *M. navarrus* (Appendix 1). The *nigricans* group had too few samples for reliable clustering when analyzed alone. However, both the morphological

648 divergence seen in male genitalia and nuclear divergence supports elevating the *M. nigricans*
649 subspecies to full species: *M. nigricans*, and *M. oregonus* **n. comb.** Based on our results, we
650 reiterate that the subspecies rank common in several groups of SRE harvestmen are conservative
651 estimates considering these "subspecies" also show fixed morphological differences that were
652 used for the initial diagnosis.

653 *Metanonychus* is a relatively ancient genus, persisting in mesic forests of the Pacific
654 Northwest since the late Oligocene, and its species are relatively old dating up to ~10 Ma with
655 extremely high levels of population divergence. From a biogeographical perspective, it is
656 interesting to note that *M. idahoensis* from northern Idaho is recovered as sister to *M. navarrus*
657 from northern California, to the exclusion of all taxa from Oregon and Washington. The break
658 between mesic forests of Idaho and coastal Oregon/Washington is found in numerous taxa
659 typically attributed to the formation of the Cascades dating to 2-5 Ma (Brunsfeld et al. 2001, and
660 references therein). Divergence dating analyses here estimate that the split between *M.*
661 *idahoensis* and *M. navarrus* is much older, dating to ~12 Ma (average K2P-corrected COI
662 divergence of 16.8%) suggesting the possibility of an older connection and divergence between
663 these regions. Further exploration of this result in the context of Pacific Northwest biogeography
664 is needed (e.g., Brunsfeld et al. 2001, Steele et al. 2005; Carstens and Richards 2007). These
665 results reaffirm the importance of SRE taxa and their inclusion in exploring and elucidating,
666 sometimes unexpected, patterns of regional biogeography and geologic history (e.g., Boyer and
667 Giribet 2009; Hedin et al. 2013; Emata and Hedin 2016).

668 **FUNDING**

This work was supported by the National Science Foundation (grant number DEB #1354558 to M.H.) and a National Science Foundation Doctoral Dissertation Improvement Grant (grant number DEB #1601208 to S.D.).

ACKNOWLEDGEMENTS

For assistance during fieldwork we thank Casey Richart, James Starrett, Alan Cabrero, Erik Ciaccio, and Morganne Sigismonti. The initial inspiration for this work was provided by Ty Roach. We thank Nick Vinciguerra for help during SNP processing and Morganne Sigismonti for assisting with initial morphological examinations. Type specimen loans were kindly provided by Darrell Ubick (California Academy of Sciences). An earlier version of the manuscript was improved through discussion with Jeet Sukumaran.

REFERENCES

Abadi M., Barham P., Chen J., Chen Z., Davis A., Dean J., Devin M., Ghemawat S., Irving G., Isard M., Kudlur M., Levenberg J., Monga R., Moores S., Murray D.G., Steiner B., Tucker P., Vasudevan V., Warden P., Wicke M., Yu Y., Zheng X. 2016. Tensorflow: a system for large-scale machine learning. *12th USENIX Symposium on Operating Systems Design and Implementation* 16:265-283. https://www.tensorflow.org/

Archer F.I., Martien K.K., Taylor B.L. 2017. Diagnosability of mtDNA with Random Forests: Using sequence data to delimit subspecies. *Mar. Mam. Sci*. 33:101-131 https://doi.org/10.1111/mms.12414

Austerlitz F., David O., Schaeffer B., Bleakley K., Olteanu M., Leblois R., Veuille M., Laredo C. 2009. DNA barcode analysis: A comparison of phylogenetic and statistical classification methods. *BMC Bioinformatics* 10:S10 https://doi.org/10.1186/1471-2105-10-S14-S10

691 Barley A.J., White J., Diesmos A.C., Brown R.M. 2013. The challenge of species delimitation at
692 the extremes: diversification without morphological change in Philippine sun skinks.
693 *Evolution* 67:3556-3572. https://doi.org/10.1111/evo.12219
694 Bauer E., Laczny C.C., Magnusdottir S., Wilmes P., Thiele I. 2015. Phenotypic differentiation of
695 gastrointestinal microbes is reflected in their encoded metabolic repertoires. *Microbiome*
696 3:55 https://doi.org/10.1186/s40168-015-0121-6
697 Blaimer B.B., Lloyd M.W., Guillory W.X., Brady S.G. 2016. Sequence capture and phylogenetic
698 utility of genomic ultraconserved elements obtained from pinned insect specimens. *PLoS*
699 *One* 11:e0161531 https://doi.org/10.1371/journal.pone.0161531
700 Blaimer B.B., LaPolla J.S., Branstetter M.G., Lloyd M.W., Brady S.G. 2016. Phylogenomics,
701 biogeography and diversification of obligate mealybug-tending ants in the genus *Acropyga*.
702 *Mol. Phylogenet. Evol.* 102:20-29 https://doi.org/10.1016/j.ympev.2016.05.030
703 Boer M.J.A., Vos R.A. Taxonomic Classification of Ants (Formicidae) from Images using Deep
704 Learning. *BioRxiv.* https://doi.org/10.1101/407452
705 Bond J.E., Stockman A.K. 2008. An integrative method for delimiting cohesion species: finding
706 the population-species interface in a group of Californian trapdoor spiders with extreme
707 genetic divergence and geographic structuring. *Syst. Biol.* 57:628-646.
708 https://doi.org/10.1080/10635150802302443
709 Bossert S., Danforth B.N. 2018 On the universality of target-enrichment baits for phylogenomic
710 research. *Methods Ecol. Evol*. 9:1453-1460 https://doi.org/10.1111/2041-210X.12988
711 Bouckaert R., Heled J., Kühnert D., Vaughan T., Wu C.H., Xie D., Suchard M.A., Rambaut A.,
712 Drummond A.J. 2014 BEAST 2: a software platform for Bayesian evolutionary analysis.
713 *PLoS Comput. Biol*. 10:e1003537 https://doi.org/10.1371/journal.pcbi.1003537

714 Boyer S.L., Baker J.M., Giribet G. 2007. Deep genetic divergences in *Aoraki denticulata*
715 (Arachnida, Opiliones, Cyphophthalmi): a widespread 'mite harvestman'defies DNA
716 taxonomy. *Mol. Ecol*. 16:4999-5016 https://doi.org/10.1111/j.1365-294X.2007.03555.x
717 Boyer S.L., Giribet G. 2009. Welcome back New Zealand: regional biogeography and
718 Gondwanan origin of three endemic genera of mite harvestmen (Arachnida, Opiliones,
719 Cyphophthalmi). *J. Biogeogr*. 36:1084-1099 https://doi.org/10.1111/j.1365-
720 2699.2009.02092.x
721 Breiman L. 1996. Bagging predictors. *Mach. Learn*. 24:123-140
722 https://doi.org/10.1007/BF00058655
723 Breiman L. 2001. Random Forests. *Mach. Learn*. 45:5–32
724 https://doi.org/10.1023/A:1010933404324.
725 Briggs T.S. 1971. The harvestmen of family Triaenonychidae in North America (Opiliones).
726 *Occas. Pap. Cal. Acad. Sci*. 90:1-43.
727 Brunsfeld, S.J., Sullivan J., Soltis D.E., Soltis P.S. 2001. Comparative phylogeography of
728 northwestern North America: a synthesis. Pages 319–339 in *Integrating ecology and*
729 *evolution in a spatial context*. (J. Silvertown and J. Antonovics, eds.). Blackwell Publishing,
730 Williston, Vermont.
731 Bryant D., Bouckaert R., Felsenstein J., Rosenberg N.A., RoyChoudhury A. 2012. Inferring
732 species trees directly from biallelic genetic markers: bypassing gene trees in a full coalescent
733 analysis. *Mol. Biol. Evol.* 29:1917-1932 https://doi.org/10.1093/molbev/mss086
734 Cao Y., Wang L. 2017 Automatic Selection of t-SNE Perplexity. arXiv:1708.03229v1 [cs.AI]
735 Campello R.J.G.B., Moulavi D., Sander J. 2013 Density-based clustering based on hierarchical
736 density estimates. In *Advances in Knowledge Discovery and Data Mining* (Pei J., Tseng V.S.,

737 Cao L., Motoda H., Xu G. eds.). PAKDD 2013. Lecture Notes in Computer Science, vol
738 7819. Springer, Berlin, Heidelberg
739 Carstens B.C., Richards C.L. 2007. Integrating coalescent and ecological niche modeling in
740 comparative phylogeography. *Evolution* 61:1439-1454 https://doi.org/10.1111/j.1558-
741 5646.2007.00117.x
742 Carstens B.C., Pelletier T.A., Reid N.M., Satler J.D. 2013. How to Fail at Species Delimitation.
743 *Mol. Ecol.* 22: 4369–4383 https://doi.org/10.1111/mec.12413
744 Castresana J. 2000. Selection of conserved blocks from multiple alignments for their use in
745 phylogenetic analysis. *Mol. Biol. Evol*. 17:540-552
746 https://doi.org/10.1093/oxfordjournals.molbev.a026334.
747 Coombes K.R., Wang M. 2018. PCDimension: Finding the Number of Significant Principal
748 Components. R package version 1.1.9
749 Chollet F. 2015 Keras. https://keras.io
750 Cordier T., Forster D., Dufresne Y., Martins C.I., Stoeck T., Pawlowski J. 2018. Supervised
751 machine learning outperforms taxonomy-based environmental DNA metabarcoding applied
752 to biomonitoring. *Mol. Ecol. Resour*. In press. https://doi.org/10.1111/1755-0998.12926
753 Danecek P., Auton A., Abecasis G., Albers C.A., Banks E., DePristo M.A., Handaker R.E.,
754 Lunter G., Marth G.T., Sherry S.T., McVean G., Durbin R., 1000 Genomes Project Analysis
755 Group. 2011. The variant call format and VCFtools. *Bioinformatics* 27:2156-2158
756 https://doi.org/10.1093/bioinformatics/btr330
757 Dayrat B. (2005) Towards integrative taxonomy. *Biol. J. Linn. Soc*. 85.:407-417
758 https://doi.org/10.1111/j.1095-8312.2005.00503.x

759 de Queiroz K. 2007. Species Concepts and Species Delimitation. *Syst. Biol.* 56:879–86
760 https://doi.org/10.1080/10635150701701083
761 Derkarabetian S., Hedin M. 2014. Integrative taxonomy and species delimitation in harvestmen:
762 a revision of the western North American genus *Sclerobunus* (Opiliones: Laniatores:
763 Travunioidea). *PloS ONE* 9:e104982. https://doi.org/10.1371/journal.pone.0104982
764 Derkarabetian S., Starrett J., Tsurusaki N., Ubick D., Castillo S., Hedin M. 2018. A stable
765 phylogenomic classification of Travunioidea (Arachnida, Opiliones, Laniatores) based on
766 sequence capture of ultraconserved elements. *ZooKeys* 760:1-36
767 https://doi.org/10.3897/zookeys.760.24937
768 DiDomenico A., Hedin M. 2016. New species in the *Sitalcina sura* species group (Opiliones,
769 Laniatores, Phalangodidae), with evidence for a biogeographic link between California desert
770 canyons and Arizona sky islands. *ZooKeys* 586:1-36
771 https://doi.org/10.3897/zookeys.586.7832
772 Donaldson J. 2016. tsne: T-Distributed Stochastic Neighbor Embedding for R (t-SNE). R
773 package version 0.1-3.
774 Earl D.A., vonHoldt B.M. 2012. STRUCTURE HARVESTER: a website and program for
775 visualizing STRUCTURE output and implementing the Evanno method. *Conserv. Genet.*
776 *Resour*. 4:359-361 https://doi.org/10.1007/s12686-011-9548-7
777 Emata K.N., Hedin M. 2016. From the mountains to the coast and back again: Ancient
778 biogeography in a radiation of short-range endemic harvestmen from California. *Mol.*
779 *Phylogenet. Evol*. 98:233-243 https://doi.org/10.1016/j.ympev.2016.02.002

780 Espíndola A., Ruffley M., Smith M.L., Carstens B.C., Tank D.C., Sullivan J. 2016 Identifying
781 cryptic diversity with predictive phylogeography. *Proc. Rol. Soc. B*. 283:20161529
782 https://doi.org/10.1098/rspb.2016.1529
783 Ester M., Kriegel H.P., Sander J., Xu X. 1996. A density-based algorithm for discovering
784 clusters in large spatial databases with noise. In *Proceedings of Second International*
785 *Conference on Knowledge Discovery and Data Mining* (Simoudis E., Han J., Fayyad U. eds.)
786 AAAI Press, Portland, Oregon, 226–231.
787 Evanno G., Regnaut S., Goudet J. 2005. Detecting the number of clusters of individuals using the
788 software STRUCTURE: a simulation study. *Mol. Ecol*. 14.:2611-2620
789 https://doi.org/10.1111/j.1365-294X.2005.02553.x
790 Ezard T.H.G., Pearson P.N., Purvis A. 2010 Algorithmic approaches to aid species' delimitation
791 in multidimensional morphospace. *BMC Evol. Biol.* 10:175 https://doi.org/10.1186/1471-
792 2148-10-175
793 Faircloth B.C. 2013. Illumiprocessor: a trimmomatic wrapper for parallel adapter and quality
794 trimming. Available from: http://dx.doi.org/10.6079/J9ILL.
795 Faircloth B.C. 2015. PHYLUCE is a software package for the analysis of conserved genomic
796 loci. *Bioinformatics* 32:786-788 https://doi.org/10.1093/bioinformatics/btv646
797 Faircloth B.C. 2017. Identifying conserved genomic elements and designing universal bait sets to
798 enrich them. *Meth. Ecol. Evol*. 8:1103-1112 https://doi.org/10.1111/2041-210X.12754
799 Fernández R., Giribet G. 2014. Phylogeography and species delimitation in the New Zealand
800 endemic, genetically hypervariable harvestman species, *Aoraki denticulata* (Arachnida,
801 Opiliones, Cyphophthalmi). *Invertebr. Syst*. 28:401-414 https://doi.org/10.1071/IS14009

802 Gnaspini P. 2007. Development. Pages 455-472 in *Harvestmen: The biology of Opiliones* (Pinto-
803 da-Rocha R., Machado G., Giribet G. eds.). Cambridge (MA) and London, England: Harvard
804 University Press.
805 Goodfellow I., Bengio Y., Courville A., Bengio Y. 2016. *Deep learning*. Cambridge (MA): MIT
806 Press.
807 Gottscho A.D., Wood D.A., Vandergast A.G., Lemos-Espinal J., Gatesy J., Reeder T.W. 2017.
808 Lineage diversification of fringe-toed lizards (Phrynosomatidae: *Uma notata* complex) in the
809 Colorado Desert: Delimiting species in the presence of gene flow. *Mol. Phylogenet. Evol.*
810 106:103-117 https://doi.org/10.1016/j.ympev.2016.09.008
811 Grabherr M.G., Haas B.J., Yassour M., Levin J.Z., Thompson D.A., Amit I., Adiconis X., Fan
812 L., Raychowdhury R., Zeng Q., Chen Z., Mauceli E., Hacohen N., Gnirke A., Rhind N., Di
813 Palma F., Birren B.W., Nusbaum C., Lindblad-Toh K., Friedman N., Regev A. 2011. Full-
814 length transcriptome assembly from RNA-Seq data without a reference genome. *Nat.*
815 *Biotechnol*. 29:644 https://doi.org/10.1038/nbt.1883
816 Guillot G., Renaud S., Ledevin R., Michaux J., Claude J. 2012. A unifying model for the analysis
817 of phenotypic, genetic, and geographic data. *Syst. Biol*. 61:897-911
818 https://doi.org/10.1093/sysbio/sys038
819 Harvey M.S. 2002. Short-range endemism amongst the Australian fauna: some examples from
820 non-marine environments. *Invertebr. Syst*. 16:555-570 https://doi.org/10.1071/IS02009
821 Harvey M.G., Smith B.T., Glenn T.C., Faircloth B.C., Brumfield R.T. 2016. Sequence capture
822 versus restriction site associated DNA sequencing for shallow systematics. *Syst. Biol*.
823 65:910-924 https://doi.org/10.1093/sysbio/syw036

824 Hedin M.C. 1997. Molecular phylogenetics at the population/species interface in cave spiders of
825 the Southern Appalachians (Araneae: Nesticidae: *Nesticus*). *Mol. Biol. Evol*. 14:309-324.
826 Hedin M. 2015. High-stakes species delimitation in eyeless cave spiders (*Cicurina*, Dictynidae,
827 Araneae) from central Texas. *Mol. Ecol*. 24:346-361 https://doi.org/10.1111/mec.13036
828 Hedin M., Starrett J., Hayashi C. 2013. Crossing the uncrossable: novel trans-valley
829 biogeographic patterns revealed in the genetic history of low-dispersal mygalomorph spiders
830 (Antrodiaetidae, *Antrodiaetus*) from California. *Mol. Ecol*. 22:508-526
831 https://doi.org/10.1111/mec.12130
832 Hedin M., Carlson D., Coyle F. 2015. Sky island diversification meets the multispecies
833 coalescent–divergence in the spruce-fir moss spider (*Microhexura montivaga*, Araneae,
834 Mygalomorphae) on the highest peaks of southern Appalachia. *Mol. Ecol*. 24:3467-3484.
835 https://doi.org/10.1111/mec.13248
836 Hedin M., Derkarabetian S., Blair J., Paquin P. 2018. Sequence capture phylogenomics of
837 eyeless *Cicurina* spiders from Texas caves, with emphasis on US federally-endangered
838 species from Bexar County (Araneae, Hahniidae). *ZooKeys* 769:49
839 https://doi.org/10.3897/zookeys.769.25814
840 Jombart T. 2008. adegenet: a R package for the multivariate analysis of genetic markers.
841 *Bioinformatics* 24:1403-1405 https://doi.org/10.1093/bioinformatics/btn129
842 Jombart T., Ahmed I. 2011 adegenet 1.3-1: new tools for the analysis of genome-wide SNP data.
843 *Bioinformatics* 27:3070-3071 https://doi.org/10.1093/bioinformatics/btr521
844 Kass R.E., Raftery A.E. 1995. Bayes factors. *J. Am. Stat. Assoc*. 90:773-795
845 Kassambara A., Mundt F. 2017. factoextra: Extract and Visualize the Results of Multivariate
846 Data Analyses. R package version 1.0.5.

847 Katoh K., Standley D.M. 2013. MAFFT multiple sequence alignment software version 7:
848 improvements in performance and usability. *Mol. Biol. Evol*. 30:772-780
849 https://doi.org/10.1093/molbev/mst010
850 Kearse M., Moir R., Wilson A., Stones-Havas S., Cheung M., Sturrock S., Buxton S., Cooper A.,
851 Markowitz S., Duran C., Thierer T., Ashton B., Meintjes P., Drummond A. 2012. Geneious
852 Basic: an integrated and extendable desktop software platform for the organization and
853 analysis of sequence data. *Bioinformatics* 28:1647-1649
854 https://doi.org/10.1093/bioinformatics/bts199
855 Kern A.D., Schrider D.R. 2018. diploS/HIC: an updated approach to classifying selective
856 sweeps. *G3-Genes Genom. Genet*. g3:200262. https://doi.org/10.1534/g3.118.200262
857 Kingma D.P., Welling M. 2013. Auto-encoding variational Bayes. In: *Proceedings of the*
858 *International Conference on Learning Representations (ICLR)*. arXiv:1312.6114v10
859 [stat.ML]
860 Kopelman N.M., Mayzel J., Jakobsson M., Rosenberg N.A., Mayrose I. 2015. Clumpak: a
861 program for identifying clustering modes and packaging population structure inferences
862 across K. *Mol. Ecol. Resour*. 15:1179-1191 https://doi.org/10.1111/1755-0998.12387
863 Leaché A.D., Koo M.S., Spencer C.L., Papenfuss T.J., Fisher R.N., McGuire J.A. (2009)
864 Quantifying ecological, morphological, and genetic variation to delimit species in the coast
865 horned lizard species complex (*Phrynosoma*). *Proc. Nat. Acad. Sci*. 106:12418-12423
866 https://doi.org/10.1073/pnas.0906380106
867 Leaché A.D., Fujita M.K., Minin V.N., Bouckaert R.R. 2014. Species delimitation using
868 genome-wide SNP data. *Syst. Biol*. 63:534-542. https://doi.org/10.1093/sysbio/syu018

869 Leaché, A.D., McElroy M.T., Trinh A. 2018 A genomic evaluation of taxonomic trends through
870 time in coast horned lizards (genus *Phrynosoma*). *Mol. Ecol.* 27(13):2884-2895
871 https://doi.org/10.1111/mec.14715
872 Li H., Durbin R. 2009. Fast and accurate short read alignment with Burrows–Wheeler transform.
873 *Bioinformatics* 25:1754-1760 https://doi.org/10.1093/bioinformatics/btp324
874 Li H., Handsaker B., Wysoker A., Fennell T., Ruan J., Homer N., Marth G., Abecasis G., Durbin
875 R., 1000 Genome Data Processing Subgroup. 2009. The sequence alignment/map format and
876 SAMtools. *Bioinformatics* 25:2078-2079 https://doi.org/10.1093/bioinformatics/btp352
877 Liaw A., Wiener M. 2002. Classification and Regression by randomForest. *R News* 2:18-22.
878 Maechler M., Rousseeuw P., Struyf A., Hubert M., Hornik K. 2018. cluster: Cluster Analysis
879 Basics and Extensions. R package version 2.0.7-1.
880 Mallet L., Bitard-Feildel T., Cerutti F., Chiapello H. 2017. PhylOligo: a package to identify
881 contaminant or untargeted organism sequences in genome assemblies. *Bioinformatics*
882 33:3283-3285 https://doi.org/10.1093/bioinformatics/btx396
883 McCormack J.E., Tsai W.L., Faircloth B.C. 2016. Sequence capture of ultraconserved elements
884 from bird museum specimens. *Mol. Ecol. Resour*. 16:1189-1203
885 https://doi.org/10.1111/1755-0998.12466
886 McInnes L., Healy, J. 2018. Umap: Uniform manifold approximation and projection for
887 dimension reduction. arXiv:1802.03426v1 [stat.ML]
888 McKenna A., Hanna M., Banks E., Sivachenko A., Cibulskis K., Kernytsky A., Garimella K.,
889 Altshuler D., Gabriel S., Daly M., DePristo M.A. 2010. The Genome Analysis Toolkit: a
890 MapReduce framework for analyzing next-generation DNA sequencing data. *Genome. Res*.
891 20:1297-1303 https://doi.org/10.1101/gr.107524.110

892 Newman C.E., Austin C.C. 2016. Sequence capture and next-generation sequencing of
893 ultraconserved elements in a large-genome salamander. *Mol. Ecol*. 25:6162-6174
894 https://doi.org/10.1111/mec.13909
895 Niemiller M.L., Near T.J., Fitzpatrick B.M. 2012. Delimiting species using multilocus data:
896 diagnosing cryptic diversity in the southern cavefish, *Typhlichthys subterraneus* (Teleostei:
897 Amblyopsidae). *Evolution* 66:846-866. https://doi.org/10.1111/j.1558-5646.2011.01480.x
898 Olteanu M., Nicolas V., Schaeffer B., Denys C., Missoup A.-D., Kennis J., Larédo C. 2013.
899 Nonlinear projection methods for visualizing barcode data and application on two data sets.
900 *Mol. Ecol. Resour.* 13:976–90 https://doi.org/10.1111/1755-0998.12047
901 Pedregosa F., Varoquaux G., Gramfort A., Michel V., Thirion B., Grisel O., Blondel M.,
902 Prettenhofer P., Weiss R., Dubourg V., Vanderplas J., Passos A., Cournapeau D., Brucher
903 M., Perrot M., Duchesney É. 2011. Scikit-learn: Machine learning in Python. *J. Mach. Learn.*
904 *Res*. 12:2825-2830
905 Pei J., Chong C., Xin L., Bin L., Yufeng W. 2018. CLADES: A classification-based machine
906 learning method for species delimitation from population genetic data. *Mol. Ecol. Resour*.
907 18:1144-1156. https://doi.org/10.1101/282608
908 Pritchard J.K., Stephens M., Donnelly P. 2000. Inference of population structure using
909 multilocus genotype data. *Genetics* 155:945-959
910 Pudlo P., Marin J.M., Estoup A., Cornuet J.M., Gautier M., Robert C.P. 2016. Reliable ABC
911 Model Choice via Random Forests. *Bioinformatics* 32:859–66
912 https://doi.org/10.1093/bioinformatics/btv684
913 R Core Team (2018) R: A Language and Environment for Statistical Computing. R Foundation
914 for Statistical Computing. Vienna, Austria. https://www.R-project.org.

915 Rousseeuw P.J. 1987. Silhouettes: a graphical aid to the interpretation and validation of cluster
916 analysis. *J. Comp. Appl. Math*. 20:53-65.
917 Ruane S., Austin C.C. 2017. Phylogenomics using formalin-fixed and 100+ year-old intractable
918 natural history specimens. *Mol. Ecol. Resour*. 17:1003-1008 https://doi.org/10.1111/1755-
919 0998.12655
920 Satler J.D., Carstens B.C., Hedin M. 2013 Multilocus Species Delimitation in a Complex of
921 Morphologically Conserved Trapdoor Spiders (Mygalomorphae, Antrodiaetidae, *Aliatypus*).
922 *Syst. Biol*. 62:805-823 https://doi.org/10.1093/sysbio/syt041
923 Schlick-Steiner B.C., Steiner F.M., Seifert B., Stauffer C., Christian E., Crozier R.H. 2010.
924 Integrative taxonomy: a multisource approach to exploring biodiversity. *Ann. Rev. Entomol.*
925 55:421-438 https://doi.org/10.1146/annurev-ento-112408-085432
926 Schrider D.R., Kern A.D. 2016. S/HIC: robust identification of soft and hard sweeps using
927 machine learning. *PLoS Genet*. 12:e1005928 https://doi.org/10.1371/journal.pgen.1005928
928 Schrider D.R., Kern A.D. 2018. Supervised machine learning for population genetics: a new
929 paradigm. *Trends Genet*. 34:301-312 https://doi.org/10.1016/j.tig.2017.12.005
930 Scrucca L., Fop M., Murphy T.B. Raftery A.E. 2017. mclust 5: clustering, classification and
931 density estimation using Gaussian finite mixture models. *The R Journal* 8/1:205-233
932 Seifert B., Ritz M., Csősz S. 2014. Application of exploratory data analyses opens a new
933 perspective in morphology-based alpha-taxonomy of eusocial organisms. *Myrmecol. News*
934 19:1-15
935 Smith B.T., Harvey M.G., Faircloth B.C., Glenn T.C., Brumfield R.T. 2013. Target capture and
936 massively parallel sequencing of ultraconserved elements for comparative studies at shallow
937 evolutionary time scales. *Syst. Biol*. 63:83-95 https://doi.org/10.1093/sysbio/syt061

938 Smith M.L., Ruffley M., Espíndola A., Tank D.C., Sullivan J., Carstens B.C. 2017. Demographic
939 model selection using random forests and the site frequency spectrum. *Mol. Ecol.* 26:4562–
940 73 https://doi.org/10.1111/mec.14223
941 Smith M.L., Carstens B.C. 2018. Disentangling the process of speciation using machine learning.
942 *BioRxiv*. https://doi.org/10.1101/356345
943 Solís-Lemus C., Knowles L.L., Ané C. 2015. Bayesian species delimitation combining multiple
944 genes and traits in a unified framework. *Evolution* 69:492-507
945 https://doi.org/10.1111/evo.12582
946 Sproul J.S., Maddison D.R. 2017. Sequencing historical specimens: successful preparation of
947 small specimens with low amounts of degraded DNA. *Mol. Ecol. Resour*. 17:1183-1201
948 https://doi.org/10.1111/1755-0998.12660
949 Srivastava N., Hinton G., Krizhevsky A., Sutskever I., Salakhutdinov R. 2014. Dropout: a simple
950 way to prevent neural networks from overfitting. *J. Mach. Learn. Res.* 15:1929-1958.
951 Stamatakis A. 2014. RAxML version 8: a tool for phylogenetic analysis and post-analysis of
952 large phylogenies. *Bioinformatics* 30:1312-1313
953 https://doi.org/10.1093/bioinformatics/btu033
954 Starrett J., Derkarabetian S., Richart C.H., Cabrero A., Hedin M. 2016. A new monster from
955 southwest Oregon forests: *Cryptomaster behemoth* sp. n. (Opiliones, Laniatores,
956 Travunioidea). *ZooKeys* 555:11-35 https://doi.org/10.3897/zookeys.555.6274
957 Starrett J., Derkarabetian S., Hedin M., Bryson Jr R.W., McCormack J.E., Faircloth B.C. 2017.
958 High phylogenetic utility of an ultraconserved element probe set designed for Arachnida.
959 *Mol. Ecol. Resour*. 17:812-823 https://doi.org/10.1111/1755-0998.12621

960 Steele C.A., Carstens B.C., Storfer A., Sullivan J. 2005. Testing hypotheses of speciation timing
961 in *Dicamptodon copei* and *Dicamptodon aterrimus* (Caudata: Dicamptodontidae). *Mol.*
962 *Phylogenet. Evol*. 36:90-100 https://doi.org/10.1016/j.ympev.2004.12.001
963 Sukumaran J., Economo E.P., Knowles L.L. 2015. Machine learning biogeographic processes
964 from biotic patterns: a new trait-dependent dispersal and diversification model with model
965 choice by simulation-trained discriminant analysis. *Syst. Biol*. 65:525-545
966 https://doi.org/10.1093/sysbio/syv121
967 Sukumaran J., Knowles L.L. 2017. Multispecies coalescent delimits structure, not species. *Proc.*
968 *Nat. Acad. Sci*. 114:1607-1612 https://doi.org/10.1073/pnas.1607921114
969 Talavera G., Castresana J. 2007. Improvement of phylogenies after removing divergent and
970 ambiguously aligned blocks from protein sequence alignments. *Syst. Biol*. 56:564-577
971 https://doi.org/10.1080/10635150701472164
972 Van der Auwera G.A., Carneiro M.O., Hartl C., Poplin R., Del Angel G., Levy-Moonshine A.,
973 Jordan T., Shakir K., Roazen D., Thibault J., Banks E., Garimella K.V., Altshuler D., Gabriel
974 S., DePristo M.A. 2013. From FastQ data to high-confidence variant calls: the genome
975 analysis toolkit best practices pipeline. *Curr. Protocol Bioinformatics* 43:11-10
976 https://doi.org/10.1002/0471250953.bi1110s43
977 Van der Maaten L.V.D., Hinton G. 2008. Visualizing data using t-SNE. *J. Mach. Learn. Res*.
978 9:2579-2605.
979 Venables W.N., Ripley B.D. 2002. Statistics and Computing. *Modern Applied Statistics with S.*
980 New York: Springer.
981 Wattenberg M., Viégas F., Johnson I. 2016. How to Use t-SNE Effectively, Distill.
982 http://doi.org/10.23915/distill

983 Weitschek E., Fiscon G., Felici G. 2014. Supervised DNA Barcodes species classification:
984 analysis, comparisons and results. *Biodata Min*. 7:4 https://doi.org/10.1186/1756-0381-7-4
985 Wiens J.J., Graham C.H. 2005. Niche conservatism: integrating evolution, ecology, and
986 conservation biology. *Ann. Rev. Ecol. Evol. Syst*. 36:519-539
987 https://doi.org/10.1146/annurev.ecolsys.36.102803.095431
988 Yang Z., Rannala B. 2010. Bayesian species delimitation using multilocus sequence data. *Proc.*
989 *Nat. Acad. Sci*. 107:9264-9269 https://doi.org/10.1073/pnas.0913022107
990 Yoshida R., Fukumizu K., Vogiatzis C. 2016. Multilocus phylogenetic analysis with gene tree
991 clustering. *Ann. Oper. Res*. 1-21. https://doi.org/10.1007/s10479-017-2456-9
992 Zarza E., Faircloth B.C., Tsai W.L., Bryson Jr R.W., Klicka J., McCormack J.E. 2016. Hidden
993 histories of gene flow in highland birds revealed with genomic markers. *Mol. Ecol*. 25:5144-
994 5157 https://doi.org/10.1111/mec.13813
995 Zarza E., Connors E.M., Maley J.M., Tsai W.L.E., Heimes P., Kaplan M., McCormack J.E.
996 2017. Combining next-generation sequencing and mtDNA data to uncover cryptic lineages of
997 Mexican highland frogs. *bioRxiv*. https://doi.org/10.1101/153601
998